Targeting the mitochondrial calcium uniporter inhibits cancer progression and alleviates cisplatin resistance in esophageal squamous cell carcinoma

YU MIAO[1*], XIAOFEI WANG[2*], YAFANG LAI[3*], YING HUANG[1], HUA YIN[1], XIANGKUN MENG[1], HAO LIU[1], RUIRUI HOU[1], WAN LIN[1], XIAOXU ZHANG[1], XU ZHANG[1], BEI CHO CHAI[1], FEIXIONG ZHANG[1], LE GUO[4] and SHAOQI YANG[1]

[1]Department of Gastroenterology, General Hospital of Ningxia Medical University, Yinchuan, Ningxia Hui Autonomous Region 750004; [2]Pathology Department, North China University of Science and Technology Affiliated Hospital, Tangshan, Hebie 063000; [3]Department of Gastroenterology, Ordos Central Hospital, Ordos, Inner Mongolia Autonomous Region 017000; [4]Department of Medical Laboratory, School of Clinical Medicine, Ningxia Medical University, Yinchuan, Ningxia Hui Autonomous Region 750004, P.R. China

Received August 13, 2022; Accepted May 5, 2023

DOI: 10.3892/ijo.2023.5530

Abstract. Cisplatin is the standard chemotherapeutic drug used for the treatment of esophageal squamous cell carcinoma (ESCC). Acquired cisplatin resistance is the primary obstacle to prolonging patient survival time. Here, the therapeutic effects of mitochondrial calcium uniporter (MCU) inhibition on tumor growth and cisplatin resistance in ESCC were assessed. MCU was stably overexpressed or knocked down in three ESCC cell lines and three cisplatin-resistant ESCC cell lines. Then, proliferation, migration, and mitochondrial membrane potential (MMP) were measured by colony formation, wound healing, Transwell, and JC-1 staining assays. MCU, MICU2, MICU1, and PD-L1 levels were detected through western blotting and immunofluorescence. ESCC and cisplatin-resistant ESCC xenograft mouse models were established. After MCU knockdown, tumor volume was measured. The expression levels of proliferation markers (CyclinD1 and Ki-67), MICU1/2, PD-L1, epithelial–mesenchymal transition (EMT) markers (vimentin, β-catenin, and E-cadherin), and the angiogenesis marker CD34 were detected through western blotting, immunohistochemistry, or immunofluorescence. The results showed that MCU overexpression significantly promoted proliferation, migration, and MMP in ESCC cells and cisplatin-resistant ESCC cells. However, proliferation, migration, and MMP were suppressed following MCU knockdown. In ESCC cells, MCU overexpression markedly increased MICU2, MICU1, and PD-L1 levels, and the opposite results were observed when MCU was stably knocked down. Similarly, MCU inhibition decreased MICU2, MICU1, and PD-L1 expression in cisplatin-resistant ESCC cells. Moreover, MCU knockdown substantially decreased tumor growth, EMT, and angiogenesis in ESCC and cisplatin-resistant ESCC xenograft mice. Collectively, targeting MCU may inhibit cancer progression and alleviate cisplatin resistance in ESCC.

Correspondence to: Professor Le Guo, Department of Medical Laboratory, School of Clinical Medicine, Ningxia Medical University, 1,160 Shengli Street, Xingqing, Yinchuan, Ningxia Hui Autonomous Region 750004, P.R. China
E-mail: guoletian1982@163.com

Professor Shaoqi Yang, Department of Gastroenterology, General Hospital of Ningxia Medical University, 804 Shengli South Street, Xingqing, Yinchuan, Ningxia Hui Autonomous Region 750004, P.R. China
E-mail: shaoqiynh@163.com

*Contributed equally

Abbreviations: ESCC, esophageal squamous cell carcinoma; MCU, mitochondrial calcium uniporter; shRNA, short hairpin RNA; NC, negative control; GFP, green fluorescent protein; HRP, horseradish peroxidase; MMP, mitochondrial membrane potential; IHC, immunohistochemistry

Key words: cisplatin resistance, esophageal squamous cell carcinoma, mitochondrial calcium uniporter, proliferation, migration, tumor growth

Introduction

Esophageal squamous cell carcinoma (ESCC) accounts for ~90% of all esophageal cancer cases and is typically in an advanced stage at the time of diagnosis (1,2). Cisplatin is the first-line chemotherapeutic agent of choice for ESCC (3). However, the development of resistance to cisplatin is a key issue hindering favorable outcomes (4). For newly treated or locally advanced ESCC patients, the initial response to cisplatin-based therapy can be as high as 50% (5). However, most patients will develop acquired cisplatin resistance, which leads to ESCC recurrence (6). Cisplatin resistance and recurrence are the primary factors leading to the failure of cisplatin therapy in OSCC patients (7). Thus, uncovering the underlying

mechanisms of cisplatin resistance and developing agents that boost sensitivity to cisplatin may provide novel therapeutic strategies.

Aberrant gene expression may be a major intrinsic factor that results in cisplatin resistance (8). Recent studies have found several molecules and signaling pathways that participate in cisplatin resistance, such as TGF-β (9), AKR1C1 (8), and the Wnt pathway (10). However, none of these have been applied in clinical practice as indicators for predicting the response to cisplatin and/or as targets in ESCC cells to improve their sensitivity to cisplatin.

Aberrations in mitochondrial Ca^{2+} homeostasis are related to various pathological processes, especially carcinogenesis (11), drug resistance (12), and cancer metastases (13). The mitochondrial calcium uniporter (MCU) complex channel [including nuclear-encoded channel-forming elements (such as MCU) and regulators (MICUs)] is a major mediator of Ca^{2+} accumulation in the mitochondrial matrix (14). Changes in the expression or function of MCU complex members are associated with various tumors and tumor-related phenotypes (15). For example, MCU-mediated mitochondrial calcium uptake facilitates tumor growth in colorectal cancer (16). MCU facilitates breast cancer growth and metastasis via HIF-1α (17). MCU-dependent mitochondrial Ca^{2+} promotes reactive oxygen species production and cancer metastases by suppressing the NAD+/SIRT3/SOD2 axis in hepatocellular carcinoma (13). However, the role of MCU in the mechanism of cisplatin resistance in ESCC remains unclear. Hence, it was hypothesized that targeting MCU may suppress tumor growth and improve cisplatin resistance in ESCC.

Materials and methods

Cell culture. In the present study, three esophageal cancer cell lines, KYSE-150, KYSE-410, and TE-1 (ATCC) were cultured in RPMI-1640 medium (Gibco; Thermo Fisher Scientific, Inc.) supplemented with 10% FBS (Gibco; Thermo Fisher Scientific, Inc.), 100 U/ml penicillin, and 100 U/ml streptomycin. Cells were maintained in a humidified incubator at 37˚C supplied with 5% CO_2 air.

Transfection. Based on the MCU sequence, two short hairpin RNAs (shRNAs) targeting MCU (sh-MCU#1 and sh-MCU#2) and one negative control shRNA (sh-NC) were designed; the sequences were: sh-MCU#1 (cat. no. PLVE2985), CCGGGATGATGTTACAGTGGTTTATCTCGAGATAAACCACTGTAACATCATCTTTTTTG; sh-MCU#2 (cat. no. PLVE2986), CCGGGACATTGGTCCAGCAACTATACTCGAGTATAGTTGCTGGACCAATGTCTTTTTTG; and sh-NC (cat. no. PLVT7) CCGGGTTCTCCGAACGTGTCACGTACTCGAGTACGTGACACGTTCGGAGAACTTTTTTG. The lentiviral vector for MCU overexpression (OE-MCU, Plasmid no. 200707HE6725-5R12) and negative control vector (OE-NC, pcDNA3.1) were purchased from Sangon Biotech, co., Ltd. Cells were treated with the overexpression vectors to construct stable MCU overexpression cells. The lentiviral plasmid (pMAGic 7.1) was purchased from Sangon Biotech, co., Ltd. Production of 3rd generation lentiviruses was performed using a ratio of lentiviral plasmid, packaging vector, and envelope of 3:2:1. A total of 42 μg lentiviral plasmid was used for transfection of 293T cells (The Chinese Academy of Sciences). Lentiviral particles were collected using an EZ-10 Spin Column Plasmid Mini-Prep Kit (Sangon Biotech, co., Ltd.). Three esophageal cancer cell lines KYSE-150, KYSE-410, and TE-1 were treated with the lentiviral particles with an MOI of 10, and incubated for 12 h. Subsequently, the medium was removed and replaced with supplemented media, and cells were cultured for a further 72 h. Puromycin (2 μg/ml) was used for the selection of stably transfected cell lines, and 1 μg/ml was used for the maintenance of stably transfected cells. Lipofectamine® 2000 (Invitrogen; Thermo Fisher Scientific, Inc.) and 200 pmol shRNA were used to transfect cells in a 60 mm dish. After mixing the shRNA, Lipofectamine® 2000, and serum-free medium, the mixture was incubated at room temperature for 20 min, added to cells, then the cells were cultured for 24 h for subsequent experimentation.

Western blotting. Cells or tissues were lysed for 20 min on ice with RIPA lysis buffer (Nanjing KeyGen Biotech Co., Ltd.) containing Sodium Deoxycholate, 1% Triton X-100, 0.1% SDS, PMSF, and protease and phosphatase inhibitors. Protein concentration was calculated using a BCA protein assay kit. A total of 30 μg protein was loaded per lane of 10% SDS-gel, resolved using SDS-PAGE, and transferred to a PVDF membrane (MilliporeSigma)/Membranes were subsequently blocked using 5% skimmed milk for 1 h at room temperature, and incubated with primary antibodies at 4˚C overnight. The primary antibodies used were: Anti-MCU (1:1,000; cat. no. sc-515930; Santa Cruz Biotechnology, Inc.), anti-MICU2 (1:1,000; cat. no. ab101465; Abcam), anti-MICU1 (1:1,000; cat. no. ab190114; Abcam), anti-PD-L1 (1:1,000; cat. no. 66248-1-Ig; ProteinTech Group, Inc.), anti-CyclinD1 (1:5,000; cat. no. 60186-1-Ig; ProteinTech Group, Inc.), anti-Ki-67 (1:1,000; cat. no. ab16667), anti-Vimentin (1:2,000; cat. no. ab92547; Abcam), anti-β-catenin (1:1,000; cat. no. 51067-2-AP; ProteinTech Group, Inc.), and anti-β-actin (1:2,000; cat. no. 20536-1-AP; ProteinTech Group, Inc.). Subsequently, the membranes were incubated with HRP-conjugated secondary antibody (1:5,000; cat. no. Zb-2301; OriGene Technologies, Inc.) at room temperature for 1 h. The bands were developed using an ECL kit (Thermo Fisher Scientific, Inc.) and analyzed using ImageJ (National Institutes of Health). β-actin served as the loading control.

Colony formation assay. The cells were plated in six-well plates ($1x10^3$ cells/well) in 2 ml supplemented media, and incubated for 14 days. Subsequently, the cells were fixed using methanol for 30 min at room temperature, followed by staining with 0.1% crystal violet at room temperature for 20 min. A total of 50 stable cells constituted a colony under an optical inverted microscope (magnification, x100). Each well was divided into three fields of view to count the number of colony.

Transwell migration assay. Cell migration was assessed using Transwell assays (Corning, Inc.). The cells were diluted to $1x10^5$/ml using serum-free RPMI-1640 medium. Then, 200 μl cell suspension was added to the upper chamber of the Transwell insert, and 600 μl medium supplemented with 20% FBS was added to the lower chamber. The cultures were incubated in a 37˚C incubator for 48 h. After removing media from the upper chamber, the cells were washed using 600 μl PBS

three times, and the cells that had migrated were stained using crystal violet at room temperature for 20 min. The number of cells that had migrated was counted using an inverted light microscope (magnification, x200) and imaged.

Wound healing assay. Cells were plated in a six-well plate ($5x10^5$ cells/well). Once a confluent monolayer had formed, a linear scratch was made in the monolayer of cells using a 200 μl pipette tip. Subsequently, the cells were washed and cultured for 48 h in supplemented serum-free RPMI-1640 media (18). Images were taken at 0 and 48 h using a light microscope (magnification, x40). The ratio of wound closure was used to quantify migration.

Measurement of the mitochondrial membrane potential (MMP). The MMP ($\Delta\psi m$) of the cells was measured using a JC-1 kit (Beyotime Institute of Biotechnology). The cells were rinsed with PBS, followed by incubation with 10 μM JC-1 at 37˚C for 30 min. Subsequently, the supernatant was aspirated. The cells were washed twice with JC-1, and 2 ml media was added. Images were acquired using a fluorescent microscope (Olympus Corporation).

Immunofluorescence staining. Cells or tissues were fixed using 4% paraformaldehyde for 20 min at room temperature, and subsequently, 0.2% Triton X-100 was added for 3 min to permeabilize cells. Non-specific binding was blocked using goat serum for 15 min at 37˚C, followed by incubation with the primary antibody against anti-MCU (1:20), anti-MICU2 (1:100), anti-MICU1 (1:100), anti-PD-L1 (1:50), or anti-CD34 (1:100; cat. no. 14486-1-AP; ProteinTech Group, Inc.) overnight at 4˚C. The following day, samples were washed with PBS three times, and the sections were incubated with Alexa Fluor® 488 Conjugate (1:100; cat. no. ZF-0512; OriGene Technologies, Inc.) or Alexa Fluor® 594 Conjugate (1:100; cat. no. ZF-0513; OriGene Technologies, Inc.) secondary antibodies at 37˚C for 2 h. Nuclei were counterstained, with DAPI (MilliporeSigma, USA) at room temperature until the samples were dry. Images were acquired using a fluorescent microscope (magnification, x400) (Olympus Corporation).

Generation of cisplatin-resistant cells. Cisplatin-resistant KYSE-150 (KYSE-150-CDDP), KYSE-410 (KYSE-410-CDDP), and TE-1 (TE-1-CDDP) cells were generated through stepwise exposure to increasing doses of cisplatin (MilliporeSigma) (19-21). Cells were first exposed to cisplatin at concentration of 5 μM for 6 months. Subsequently, the cells were maintained in cisplatin-free RPMI-1640 medium for 3 days. When confluence reached the initial confluence prior to treatment, the cells were treated with a higher concentration of cisplatin (10, 20, 40, or 60 μM). The concentration was gradually elevated every few passages until a concentration of 60 μM was reached (within 2 months). For subsequent maintenance of cisplatin resistance in cells, 60 μM cisplatin was used in general culture.

Mouse xenograft models. BALB/c nude male mice (weighing 16-20 g, 5 weeks old; Beijing Vital River Laboratory Animal Technology Co., Ltd.) were kept at 24±2˚C, in a humid environment (60±10%), with a 12/12 light-dark cycle, and free access to food and water. The mice were randomly separated into four groups (n=5 per group). The mice were subcutaneously injected with sh-NC-transfected KYSE-150 cells (Control), sh-NC-transfected KYSE-150-CDDP cells (CDDP), sh-MCU-transfected KYSE-150 cells (sh-MCU), or sh-MCU-transfected KYSE-150-CDDP cells (CDDP+sh-MCU) ($2x10^6$ in 0.1 ml) in the back. The tumor volumes were measured weekly using the following formula: volume=0.5x length x width^2. After 21 days, mice were euthanized by cervical dislocation following anesthesia by injection of sodium pentobarbital (50 mg/kg) intraperitoneally, and the tumors were isolated, weighed, and prepared for subsequent analysis. The protocol used strictly adhered to the Guidelines for the Care and Use of Laboratory Animals, and was approved by the Ethics Committee of Ningxia Medical University (approval no. 2020-880).

Immunohistochemistry (IHC) staining. Tissues from the subcutaneous tumors of nude mice were collected and fixed in 10% neutral formalin solution at room temperature for 24 h. The xenograft tumors were collected and embedded in paraffin, sectioned into 4 μm slices, dewaxed, repaired under high pressure for 3 min in EDTA (ZLI-9072; ZSGB-BIO), incubated with 3% hydrogen peroxide at 37˚C for 15 min as a quenching step, then blocked with 10% goat serum at 37˚C for 30 min. Then, the sections were incubated with primary antibodies at 4˚C overnight. The primary antibodies used were: Anti-MCU (1:20; sc-515930; SANTA CRUZ, USA), anti-MICU2 (1:100), anti-MICU1 (1:100), anti-PD-L1 (1:100), anti-Ki-67 (1:100), anti-Vimentin (1:150; cat. no. 10366-1-AP; ProteinTech Group, Inc.), or anti-E-cadherin (1:100; cat. no. 20874-1-AP; ProteinTech Group, Inc.). The sections were stained with HRP-conjugated secondary antibodies (cat. no. PV-9000; OriGene Technologies, Inc.) at room temperature for 1 h followed by DAB chromogenic solution, and counterstaining with hematoxylin at room temperature for 3 min. Samples were finally sealed, and imaged using a microscope (magnification, x400) (BX61, Olympus Corporation), and analyzed using IPP version 6.0 (Media Cybernetics).

Reverse transcription-quantitative PCR (RT-qPCR). Total RNA was isolated from KYSE-150, KYSE-410, and TE-1 cells using TRIzol®. RevertAid First Strand cDNA Synthesis Kit (Thermo Fisher Scientific, Inc.) was used to synthesize cDNA [using 5 μg RNA, 1 μl Oligo(dT)18 primer (100 μM), 1 μl Random Hexamer primers (100 μM), 4 μl 5x Reaction Buffer, 1 μl RiboLock RNase Inhibitor (20 U/μl), 2 μl dNTP Mix (10 mM), and 1 μl RevertAid M-MuLV RT (200 U/μl), made to a final volume of 20 μl using nucleotide-free water]. PowerUp™ SYBR™ Green MasterMix (Applied Biosystems, Thermo Fisher Scientific, Inc.) was used for qPCR. The thermocycling conditions were: 20 sec initial denaturation at 95˚C; followed by 35 cycles of 1 sec at 95˚C for denaturation, and 20 sec at 60˚C for annealing and extension. The primers were designed by Sangon Biotech, Co., Ltd., and the sequences were: MCU forward, 5'-TCCAGAAGCCAGAGACAGAC-3' and reverse, 5'-TGTCGGAGAGGCAGATGTAC-3'. GAPDH forward, 5'-CAAGGTCATCCATGACAACTTTG-3' and reverse, 5'-GTCCACCACCCTGTTGCTGTAG-3'. GAPDH was used as the housekeeping gene. Gene expression was normalized using the $2^{-\Delta\Delta Cq}$ method (22).

Statistical analysis. All statistical analysis was performed using SPSS version 22.0 (IBM Corp.). Each assay was performed in triplicate. Data are presented as the mean ± SD. Differences between ≥3 groups were compared using a one-way ANOVA followed by Bonferroni corrections. $P<0.05$ was considered to indicate a statistically significant difference.

Results

MCU increases the proliferative capacity of ESCC cells. To investigate the biological role of MCU on ESCC progression, MCU was stably overexpressed or knocked down in three ESCC cell lines (KYSE-150, KYSE-410, and TE-1 cells; Fig. 1A and B). The transfection efficacy was confirmed using western blotting and RT-qPCR. The results showed that transfection of the OE-MCU vector resulted in overexpression of MCU at the protein and mRNA level in KYSE-150, KYSE-410, and TE-1 cells (Figs. 1C-F and S1D-F). Moreover, both sh-MCU#1 and sh-MCU#2 significantly reduced MCU protein and mRNA expression levels compared with the sh-NC transfected cells in all three ESCC cell lines (Figs. 1G-J and S1A-C). These results indicated that MCU was separately successfully overexpressed as well as knocked down in the ESCC cells. the proliferative capacity of ESCC cells was determined using a colony formation assay; MCU overexpression significantly increased the proliferation of KYSE-150, KYSE-410, and TE-1 cells (Fig. 1K-P). Conversely, MCU knockdown substantially decreased the proliferation of ESCC cells. These results suggested that MCU regulated the proliferation of ESCC cells.

MCU facilitates the acquisition of metastatic phenotypes and the MMP of ESCC cells. The effect of MCU on cell migration and invasion was investigated using Transwell and wound healing assays. The results of the Transwell assays showed that stably overexpressed MCU significantly increased cell migration of KYSE-150, KYSE-410, and TE-1 cells (Fig. 2A-D). Conversely, MCU knockdown substantially reduced the migratory capacity of the ESCC cell lines (Fig. 2A-D). Furthermore, the wound healing assay showed that MCU overexpression significantly increased wound closure in all three cell lines (Fig. 2E-H). In contrast, wound closure was significantly reduced following MCU knockdown. Using JC-1 staining, the MMP was investigated in the three cell lines. MCU overexpression markedly increased the MMP (Fig. 2I-L), whereas MCU knockdown resulted in a significant decrease in the MMP of cells. Collectively, these results indicated that MCU regulated the acquisition of a metastatic phenotype and the MMP of ESCC cells, suggesting that the effect of MCU on ESCC cell metastasis is associated with its ability to modulate the MMP.

MCU increases MICU2, MICU1, and PD-L1 expression in ESCC cells. The regulatory roles of MCU on MICU2, MICU1, and PD-L1 expression were determined through western blotting. In KYSE-150 cells, MCU overexpression markedly increased the expression of MICU2, MICU1, and PD-L1. In contrast, MICU2, MICU1, and PD-L1 expression was significantly reduced when MCU expression was knocked down the three ESCC cell lines (Fig. S2). Immunofluorescence analysis was used to determine whether MCU affected MICU2, MICU1, and PD-L1 expression. Consistent with the results of western blotting, MCU overexpression significantly increased MICU2, MICU1, and PD-L1 expression in the three cell lines (Figs. 3 and S3). In contrast, following MCU knockdown, MICU2, MICU1, and PD-L1 expression was significantly decreased. Thus, MCU increased MICU1, MICU2, and PD-L1 expression in ESCC cells, suggesting a possible regulatory association between MCU and PD-L1.

MCU overexpression upregulates MICU2, MICU1, and PD-L1 expression in cisplatin-resistant ESCC cells. Here, cisplatin-resistant KYSE-150 (KYSE-150-CDDP), KYSE-410 (KYSE-410-CDDP), and TE-1 (TE-1-CDDP) cells were established through a stepwise increase in exposure to higher concentrations of cisplatin. In cisplatin-resistant ESCC cells, the effects of MCU on MICU2, MICU1, and PD-L1 expression were assessed. Western blotting confirmed that MCU was stably overexpressed and knocked down in KYSE-150-CDDP cells (Fig. 4A and B). Moreover, MCU overexpression substantially increased the expression of MICU2, MICU1, and PD-L1 in KYSE-150-CDDP cells (Fig. 4C-E). Conversely MCU knockdown substantially decreased the expression of MICU2, MICU1, and PD-L1 in KYSE-150-CDDP cells. Similar results were also observed in KYSE-410-CDDP (Fig. 4F-J) and TE-1-CDDP cells (Fig. 4K-O). Immunofluorescence analysis was performed to observe the influence of MCU on MICU2, MICU1, and PD-L1 expression in cisplatin-resistant ESCC cells. The data confirmed that MCU overexpression markedly increased MICU2, MICU1, and PD-L1 expression in KYSE-150-CDDP (Fig. 5A-E), KYSE-410-CDDP (Fig. 5F-J), and TE-1-CDDP cells (Fig. 5K-O). In contrast, MCU knockdown significantly decreased MICU1, MICU2, and PD-L1 expression in cisplatin-resistant ESCC cells. The regulatory relationship between MCU and PD-L1 was also observed in the cisplatin-resistant ESCC cells.

MCU knockdown decreases the proliferation and MMP of cisplatin-resistant ESCC cells. The role of MCU on cisplatin resistance was further investigated in cisplatin-resistant ESCC cells. The results of the colony formation assays showed that MCU overexpression significantly enhanced the proliferative capacity of cisplatin-resistant KYSE-150, KYSE-410, and TE-1 cells (Fig. 6A-D). Conversely, MCU knockdown significantly reduced the proliferative ability of KYSE-150-CDDP, KYSE-410-CDDP, and TE-1-CDDP cells. As shown in Fig. 6E-H, the MMP of KYSE-150-CDDP, KYSE-410-CDDP, and TE-1-CDDP cells was markedly increased by MCU overexpression. In contrast, MCU knockdown significantly reduced the MMP of cisplatin-resistant ESCC cells.

MCU inhibition reduces the migration of cisplatin-resistant ESCC cells. The effects of MCU on the migratory capacity of cisplatin-resistant ESCC cells were observed using wound healing and Transwell assays. As shown in Fig. 7A-D, MCU upregulation significantly increased wound closure of KYSE-150-CDDP, KYSE-410-CDDP, and TE-1-CDDP cells. Conversely, MCU knockdown significantly decreased wound closure in the cisplatin-resistant ESCC cells. The results of the Transwell assays also showed that MCU overexpression

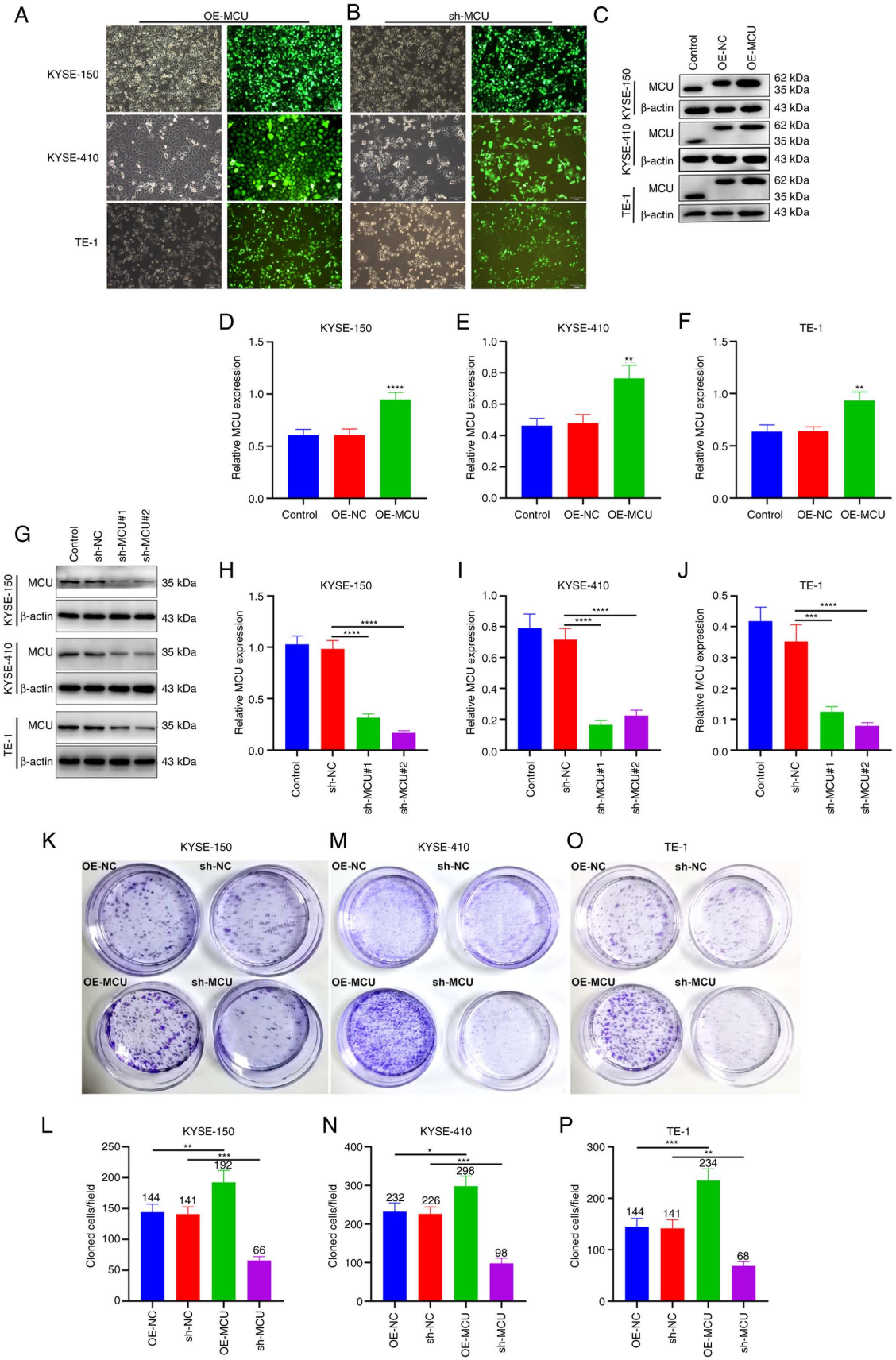

Figure 1. MCU accelerates the proliferative capacity of ESCC cells. (A and B) Construction of MCU-overexpressing or MCU-knockdown KYSE-150, KYSE-410, and TE-1 cells. GFP-PURO-MCU transfection was observed using a fluorescent microscope (magnification, x100). Scale bar, 100 μm. (C-F) MCU expression was examined in MCU-overexpressing KYSE-150, KYSE-410, and TE-1 cells by western blotting. **P<0.01, ****P<0.0001 vs. OE-NC group. (G-J) KYSE-150, KYSE-410, and TE-1 cells were transfected with shRNAs targeting MCU or sh-NC for 48 h, and MCU expression was detected by western blot. ***P<0.001, ****P<0.0001 vs. sh-NC group. (K-P) Following stable overexpression or knockdown of MCU in KYSE-150, KYSE-410, and TE-1 cells, the proliferative capacity was assessed using a colony formation assay. *P<0.05, **P<0.01, ***P<0.001 vs. OE-NC or sh-NC group. Data are presented as the mean ± SD. MCU, mitochondrial calcium uniporter; ESCC, esophageal squamous cell carcinoma; PURO, puromycin; OE, overexpression; shRNA, short hairpin RNA; NC, negative control.

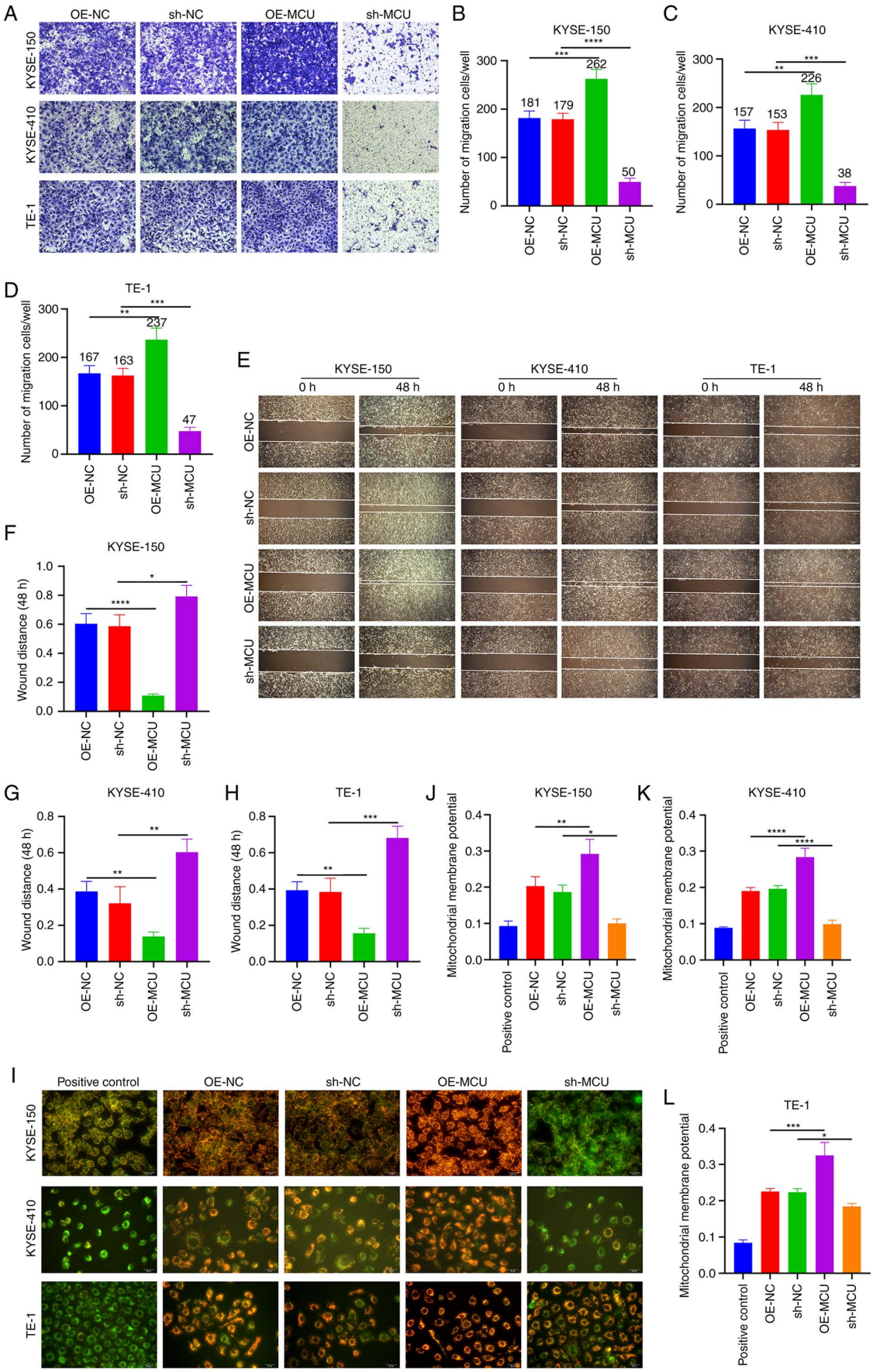

Figure 2. MCU facilitates a metastatic phenotype and regulates the MMP of ESCC cells. (A-D) MCU was stably overexpressed or knocked down in KYSE-150, KYSE-, and TE-1 cells. The migration of cells was assessed using Transwell assays. Scale bar, 50 μm. (E-H) Wound healing assays were performed using the established ESCC cells. Scale bar, 200 μm. (I-L) The MMP was detected in the established ESCC cells. Scale bar, 20 μm. n=3. Data are presented as the mean ± SD. *P<0.05, **P<0.01, ***P<0.001, ****P<0.0001. MCU, mitochondrial calcium uniporter; ESCC, esophageal squamous cell carcinoma; MMP, mitochondrial membrane potential; OE, overexpression; shRNA, short hairpin RNA; NC, negative control.

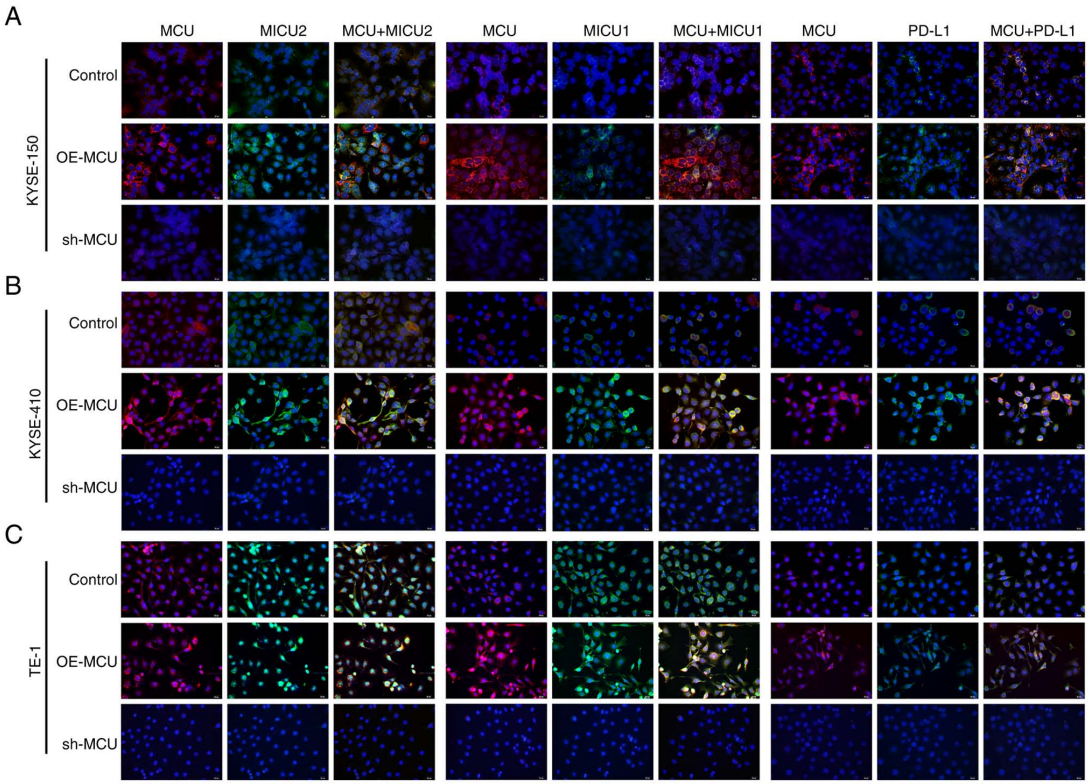

Figure 3. MCU increases MICU1, MICU2, and PD-L1 expression in ESCC cells. (A-C) Immunofluorescence analysis was used to detect the expression of MCU, MICU1, MICU2, and PD-L1 in KYSE-150, KYSE-410, and TE-1 with MCU overexpressed or knocked down. Scale bar, 20 μm. MCU, mitochondrial calcium uniporter; ESCC, esophageal squamous cell carcinoma.

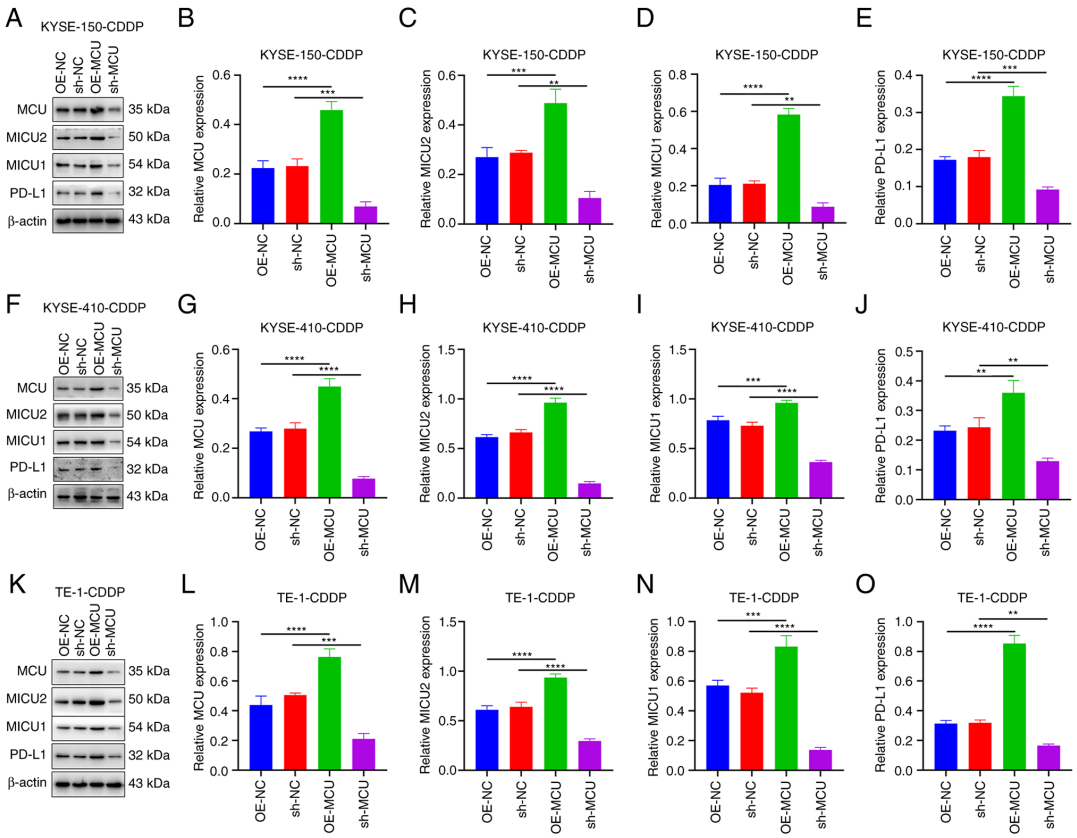

Figure 4. MCU overexpression upregulates MICU1, MICU2, and PD-L1 expression in cisplatin-resistant ESCC cells. (A-O) Western blotting was used to determine the expression of MCU, MICU1, MICU2, and PD-L1 expression in cells overexpressing or knocked down KYSE-150-CDDP, KYSE-410-CDDP, and TE-1-CDDP cells. Data are presented as the mean ± SD. **P<0.01, ***P<0.001, ****P<0.0001. MCU, mitochondrial calcium uniporter; ESCC, esophageal squamous cell carcinoma; CDDP, cisplatin-resistant; OE, overexpression; shRNA, short hairpin RNA; NC, negative control.

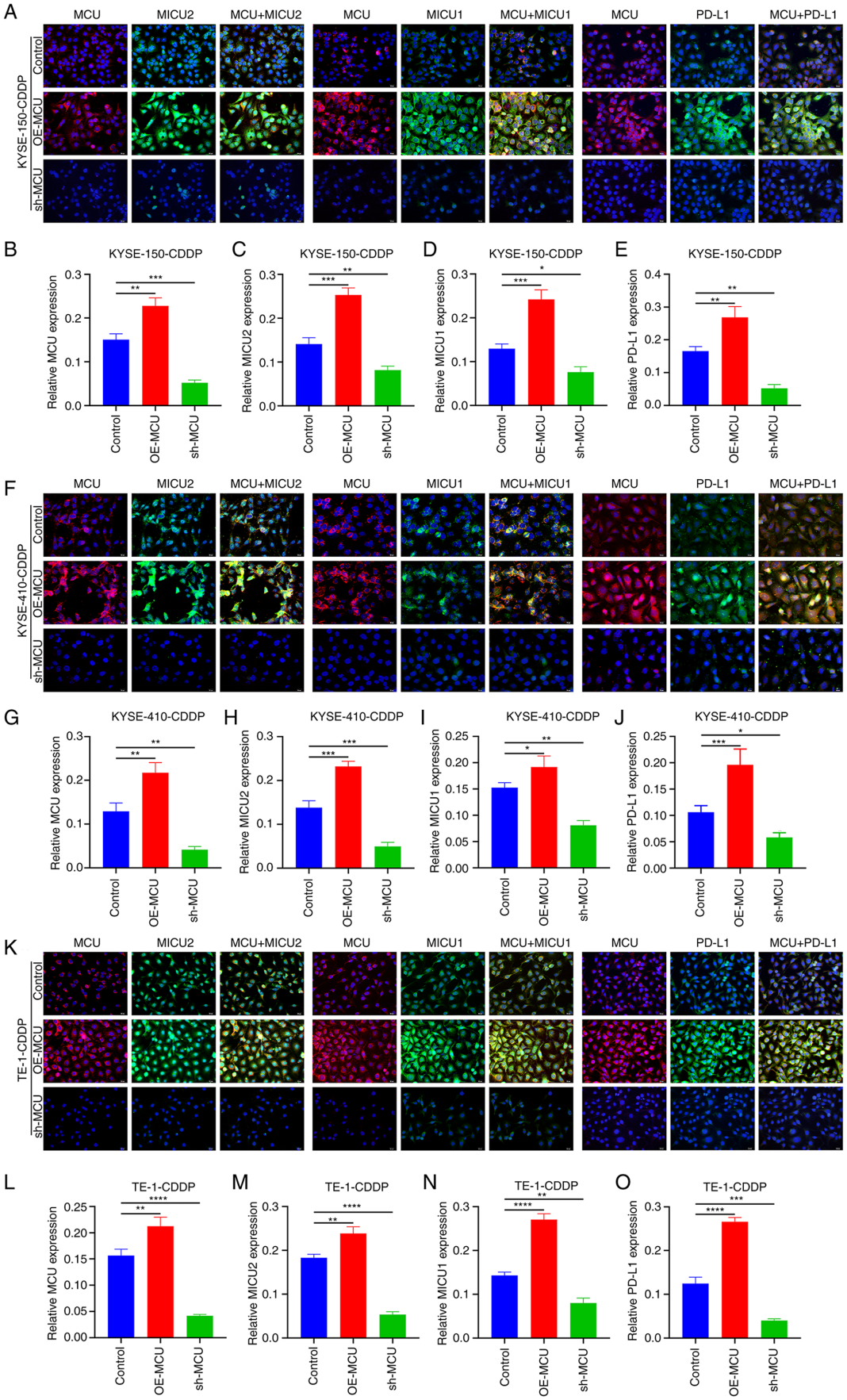

Figure 5. The effects of MCU on MICU1, MICU2, and PD-L1 expression in cisplatin-resistant ESCC cells. When MCU was stably overexpressed or knocked down, immunofluorescence analysis was used to determine the expression of MCU, MICU1, MICU2, and PD-L1 expression in (A-E) KYSE-150-CDDP, (F-J) KYSE-410-CDDP, and (K-O) TE-1-CDDP cells. Scale bar, 20 μm. Data are presented as the mean ± SD. *P<0.05, **P<0.01, ***P<0.001, ****P<0.0001. MCU, mitochondrial calcium uniporter; ESCC, esophageal squamous cell carcinoma; CDDP, cisplatin-resistant; Ns, not significant; OE, overexpression; shRNA, short hairpin RNA; OE, overexpression; shRNA, short hairpin RNA.

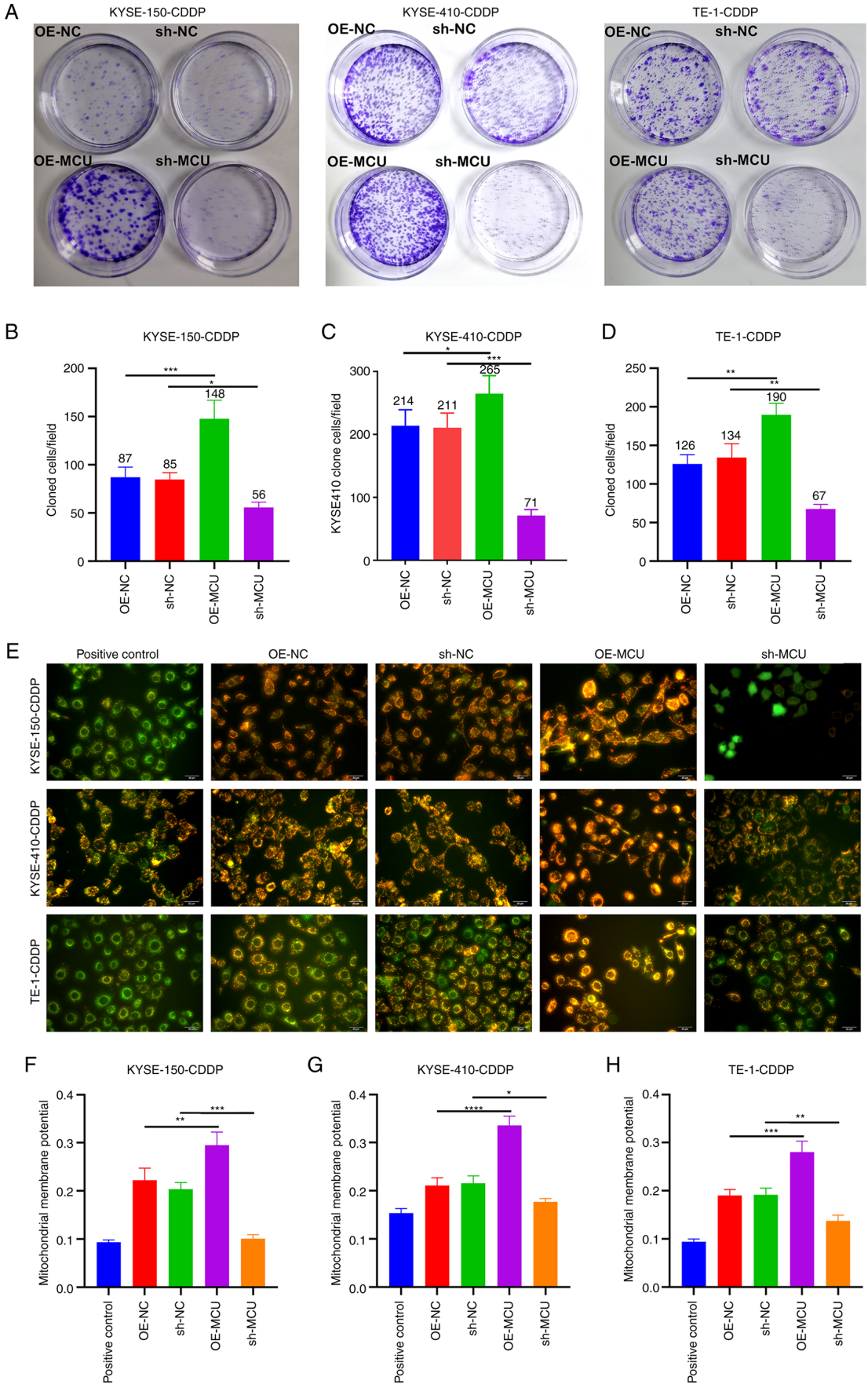

Figure 6. MCU inhibition reduces the proliferation and MMP of cisplatin-resistant ESCC cells. (A-D) MCU was stably overexpressed or knocked down, and the proliferative capacities of KYSE-150-CDDP, KYSE-410-CDDP, and TE-1-CDDP cells were evaluated using colony formation assays. (E-H) The mitochondrial membrane potential was determined in KYSE-150-CDDP, KYSE-410-CDDP, and TE-1-CDDP cells in which MCU had been overexpressed or knocked down. Scale bar, 20 μm. Data are presented as the mean ± SD of three repeats. *P<0.05, **P<0.01, ***P<0.001, ****P<0.0001. MCU, mitochondrial calcium uniporter; ESCC, esophageal squamous cell carcinoma; CDDP, cisplatin-resistant; OE, overexpression; shRNA, short hairpin RNA.

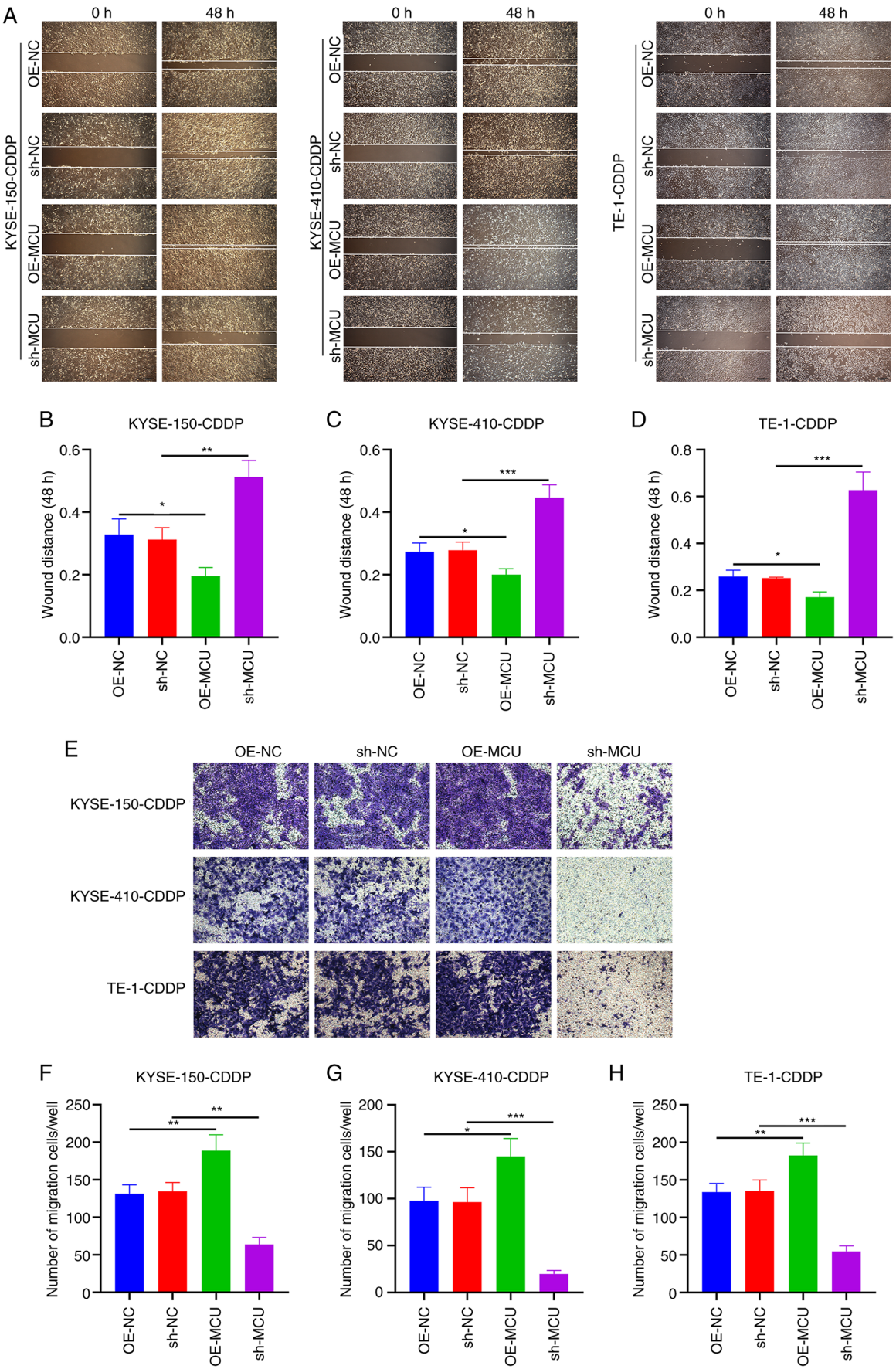

Figure 7. MCU knockdown decreased the migratory capacity of cisplatin-resistant ESCC cells. (A-D) MCU was stably overexpressed or knocked down, and wound healing was measured in KYSE-150-CDDP, KYSE-410-CDDP, and TE-1-CDDP cells. Scale bar, 200 μm. (E-H) Transwell migration assays were performed on the MCU overexpressing or MCU knocked down KYSE-150-CDDP, KYSE-410-CDDP, and TE-1-CDDP cells. Scale bar, 50 μm. Data are presented as the mean ± SD. *P<0.05, **P<0.01, ***P<0.001. MCU, mitochondrial calcium uniporter; ESCC, esophageal squamous cell carcinoma; CDDP, cisplatin-resistant; OE, overexpression; shRNA, short hairpin RNA.

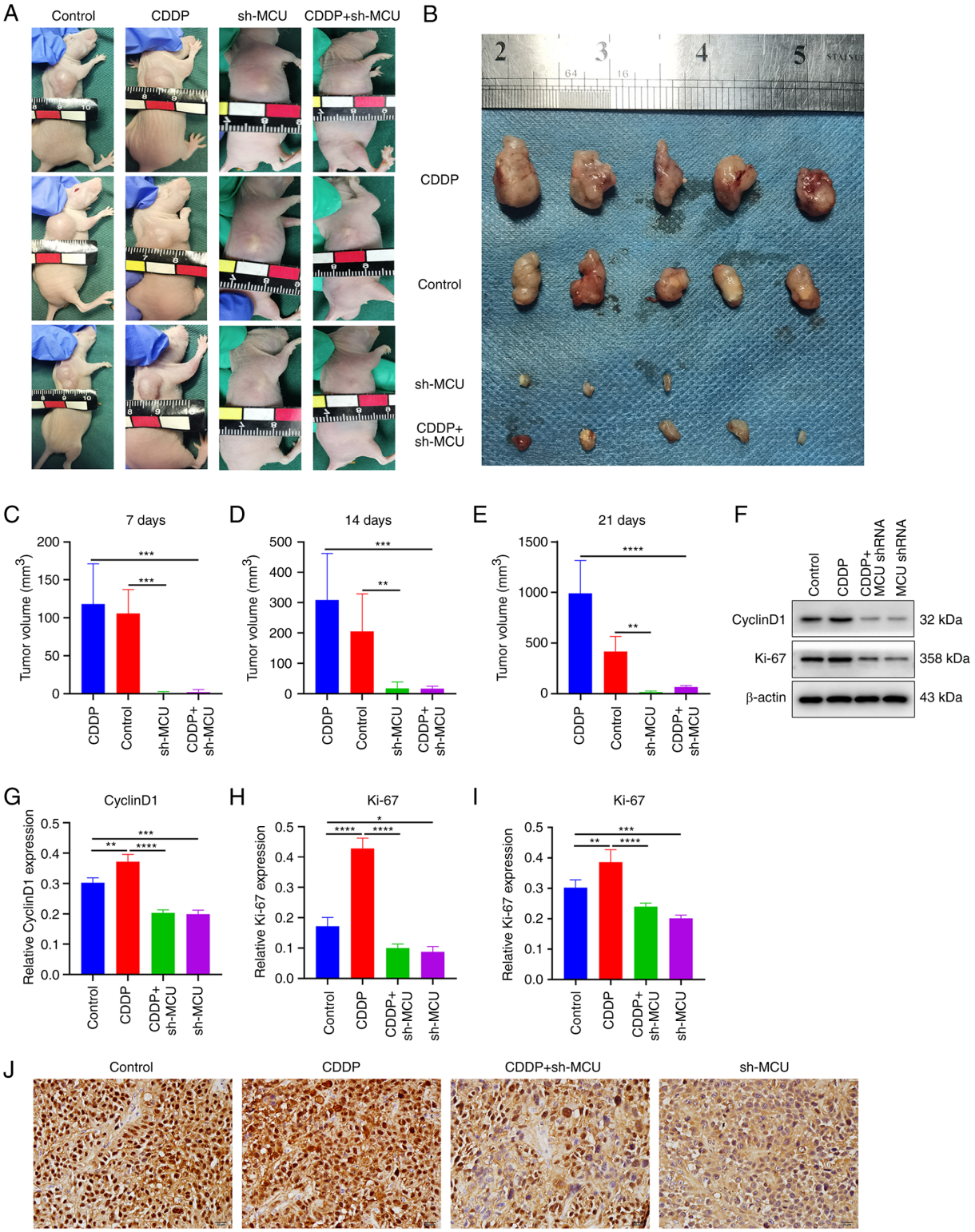

Figure 8. MCU knockdown reduced tumor growth and cisplatin resistance in ESCC xenograft mouse models. (A) BALB/c nude mice were subcutaneously injected with sh-NC-transfected KYSE-150 cells (Control), sh-NC-transfected KYSE-150-CDDP cells (CDDP), sh-MCU-transfected KYSE-150 cells (sh-MCU), or sh-MCU-transfected KYSE-150-CDDP cells (CDDP+sh-MCU) (n=5 each group). Images of xenograft mice were acquired 21 days following the injection of cells. (B) Representative images of tumors removed after 21 days. (C-E) Tumor volume was measured on days 7, 14, and 21 after the injection of cells. (F-H) CyclinD1 and Ki-67 expression was detected in the dissected tumors using western blotting. (I and J) Ki-67 expression was examined in the dissected tumors by immunohistochemistry. Scale bar, 20 μm. Data are presented as the mean ± SD. *P<0.05, **P<0.01, ***P<0.001, ****P<0.0001. MCU, mitochondrial calcium uniporter; ESCC, esophageal squamous cell carcinoma; OE, overexpression; shRNA, short hairpin RNA.

significantly increased the number of KYSE-150-CDDP, KYSE-410-CDDP, and TE-1-CDDP cells that had migrated (Fig. 7E-H); the opposite results were observed when MCU was stably knocked down in the cisplatin-resistant ESCC cells. The migratory and invasive abilities of cisplatin-resistant and non-cisplatin-resistant ESCC cells were compared, and the

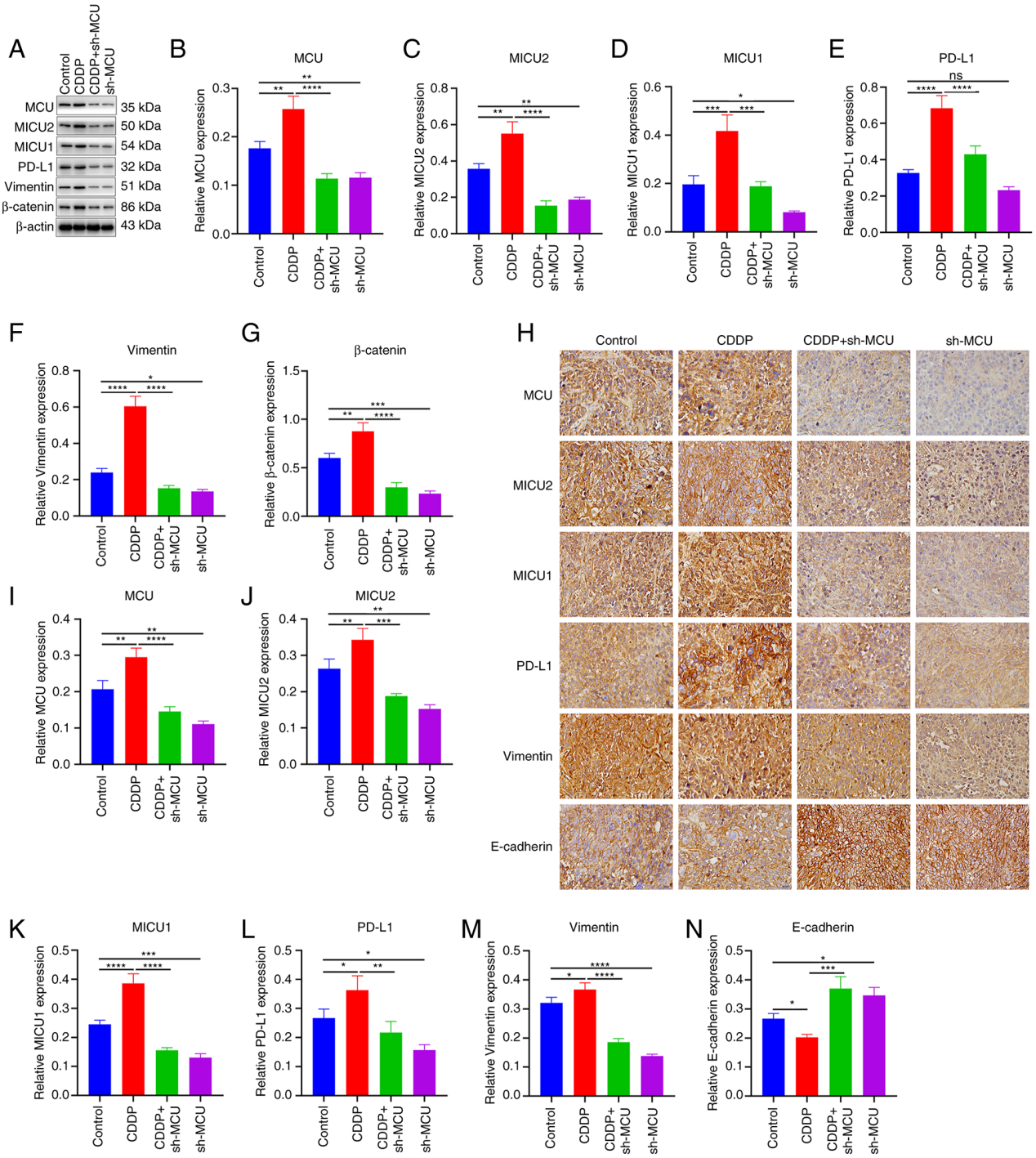

Figure 9. MCU knockdown decreased MICU1, MICU2, and PD-L1 expression, and abrogated EMT in cisplatin-resistant ESCC xenograft mice. (A-G) MCU, MICU1, MICU2, PD-L1, Vimentin, and β-catenin expression was detected in sh-NC-transfected KYSE-150 (Control), sh-NC-transfected KYSE-150-CDDP (CDDP), sh-MCU-transfected KYSE-150 (sh-MCU), or sh-MCU-transfected KYSE-150-CDDP (CDDP+sh-MCU) cell-xenograft tumors using western blotting. (H-N) MCU, MICU1, MICU2, PD-L1, Vimentin, and E-cadherin expression was determined in Control, CDDP, sh-MCU, and CDDP+sh-MCU cell-xenograft tumors by IHC. Scale bar, 20 μm. Data are presented as the mean ± SD. *P<0.05, **P<0.01, ***P<0.001 ****P<0.0001. MCU, mitochondrial calcium uniporter; ESCC, esophageal squamous cell carcinoma; OE, overexpression; shRNA, short hairpin RNA.

results showed that the invasive and migration capacity of cisplatin-resistant ESCC cells was not significantly increased, but decreased compared with the non-cisplatin-resistant cells. Interestingly, overexpression or knockdown of MCU also regulated the invasive and migration capacity of cisplatin-resistant cells (Fig. S4). These results further suggest that MCU plays an important role in the metastasis of cisplatin-resistant and non-cisplatin-resistant ESCC cells.

MCU knockdown suppresses tumor growth and cisplatin resistance in ESCC xenograft mice. BALB/c nude mice were subcutaneously injected with sh-NC-transfected KYSE-150 cells, sh-NC-transfected KYSE150-CDDP cells, sh-MCU-transfected KYSE-150 cells, or sh-MCU-transfected KYSE-150-CDDP cells ($2x10^6$ cells in 0.1 ml) in the back (n=5 per group). The tumor volumes were determined on days 7, 14, and 21. Mice were euthanized on day 21 after

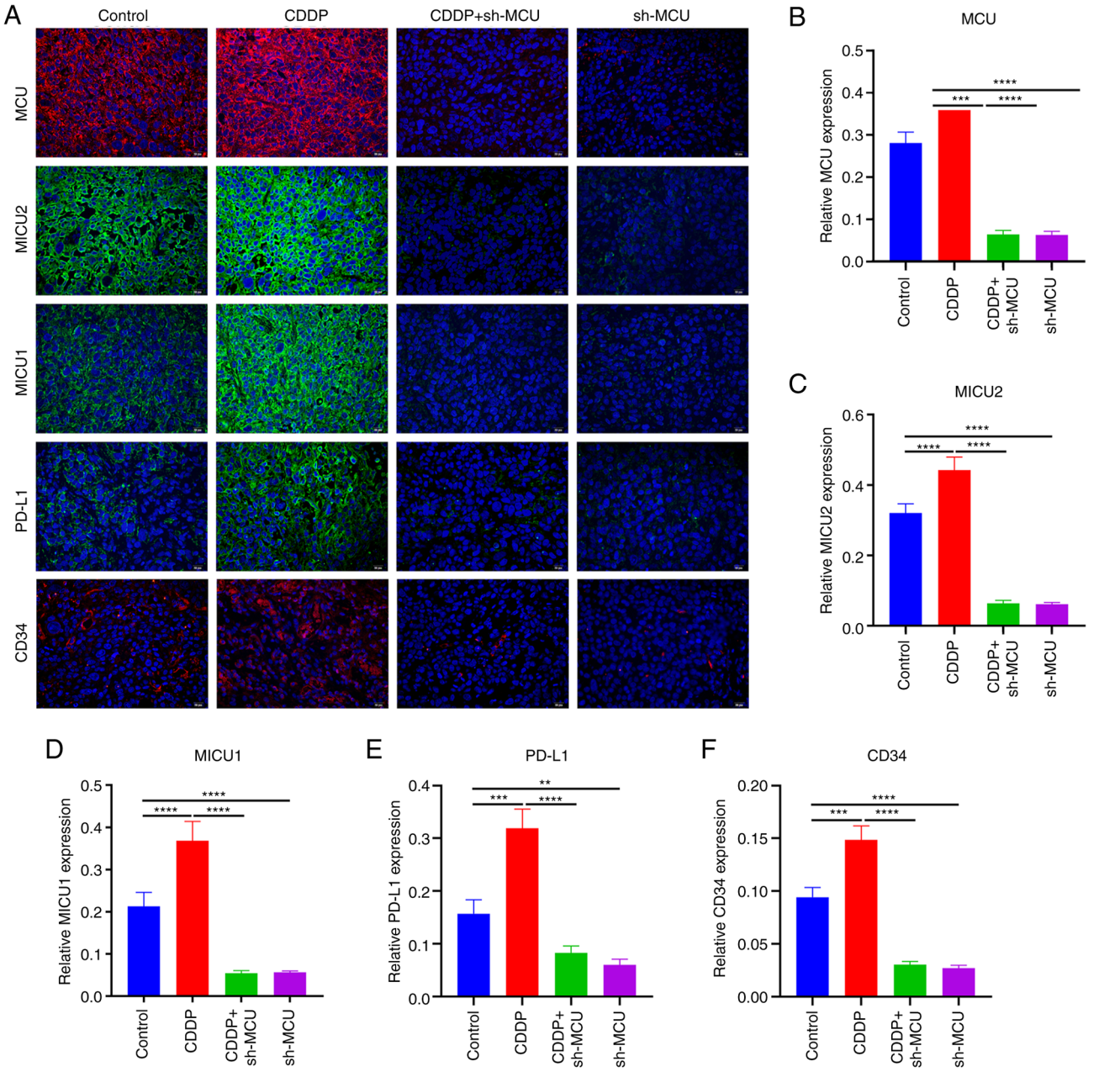

Figure 10. MCU knockdown decreases MICU1, MICU2, PD-L1, and CD34 expression in cisplatin-resistant ESCC xenograft mice. (A-F) MCU, MICU1, MICU2, PD-L1, and CD34 expression were determined using immunofluorescence analysis. Scale bar, 20 μm Data are presented as the mean ± SD. **P<0.01, ***P<0.001, ****P<0.0001. OE, overexpression; shRNA, short hairpin RNA; MCU, mitochondrial calcium uniporter; CDDP, cisplatin-resistant.

inoculation of cells. The results showed that MCU knockdown significantly reduced the tumor volume both in KYSE-150 and KYSE-150-CDDP cell xenograft mice (Fig. 8A-E). The expression of proliferation markers CyclinD1 and Ki-67 was examined in the dissected tumors using western blotting. Expression of CyclinD1 and Ki-67 was significantly increased in cisplatin-resistant ESCC xenograft tumors compared with the ESCC xenograft tumors (Fig. 8F-H). MCU knockdown substantially reduced the expression of CyclinD1 and Ki-67 both in ESCC xenograft tumors and cisplatin-resistant ESCC xenograft tumors. Similar findings were observed regarding Ki-67 expression suing IHC (Fig. 8I and J). Thus, MCU knockdown significantly reduced tumor growth in cisplatin-resistant and non-cisplatin-resistant ESCC cell xenograft mice.

MCU knockdown reduces MICU2, MICU1, and PD-L1 expression and EMT in cisplatin-resistant ESCC xenograft mice. Using western blotting, the expression of MCU, MICU2, MICU1, PD-L1, and EMT markers (Vimentin and β-catenin) was assessed in xenograft tumors. Compared with the ESCC xenograft tumors, MCU, MICU2, MICU1, PD-L1, Vimentin, and β-catenin exhibited higher expression in cisplatin-resistant ESCC xenograft tumors (Fig. 9A-G). MCU inhibition reduced the expression of MCU, MICU2, MICU1, PD-L1, Vimentin, and β-catenin both in ESCC xenograft tumors and cisplatin-resistant ESCC xenograft tumors (Fig. 9A-G). IHC analysis also showed that the expression of MCU, MICU2, MICU1, PD-L1, and Vimentin expression was significantly increased, whilst E-cadherin expression was significantly

decreased in cisplatin-resistant ESCC xenograft tumors compared with the ESCC xenograft tumors (Fig. 9H-N). MCU inhibition significantly reduced the expression of MCU, MICU2, MICU1, PD-L1, and Vimentin, but increased E-cadherin expression both in ESCC xenograft tumors and cisplatin-resistant ESCC xenograft tumors. These results were confirmed using immunofluorescence analysis (Fig. 10). Thus, MCU knockdown reduced MICU2, MICU1, and PD-L1 expression, and abrogated EMT in cisplatin-resistant and non-cisplatin-resistant ESCC xenografts.

MCU knockdown reduces angiogenesis in cisplatin-resistant ESCC in vivo. Using immunofluorescence analysis, the expression of CD34 (an indicator of microvessel density in xenograft tumors) was detected. The results showed that CD34 expression was increased in cisplatin-resistant ESCC xenograft tumors when compared with normal ESCC xenograft tumors (Fig. 10A and F). MCU inhibition substantially decreased the expression of CD34 both in ESCC xenograft tumors and cisplatin-resistant ESCC xenograft tumors. Thus, the results data indicated that MCU knockdown may inhibit angiogenesis in cisplatin-resistant and non-cisplatin-resistant ESCC xenograft mice.

Discussion

Cisplatin-based regimens have been routinely applied for the treatment of patients with ESCC (19). However, the administration of cisplatin is typically accompanied by the development of cisplatin resistance (23). Understanding the mechanisms underlying the acquisition of cisplatin resistance may enable the development of more effective treatment schemes, thereby overcoming chemotherapy resistance and improving ESCC clinical outcomes (24-26). A tumor is a heterogeneous cell mixture that harbors multiple genetic variations and gene expression patterns (27,28). In the present study, it was demonstrated that targeting MCU suppressed tumor growth and decreased PD-L1 expression in both cisplatin-resistant and non-cisplatin-resistant ESCC cells. In future studies, additional ESCC cell lines and subcutaneous tumor models of esophageal cancer cells in nude mice will be used to elucidate the molecular regulatory mechanism of reversing cisplatin resistance through MUC knockout.

In three ESCC cell lines, MCU overexpression markedly enhanced proliferation, migration, and MMP, and the opposite results were observed when MCU was stably knocked down. The carcinogenic effects of MCU have been reported in various types of cancer. As an example, MCU facilitates migration, invasion, angiogenesis, and tumor growth of gastric cancer (29). Here, the therapeutic effects of MCU inhibition were also confirmed in cisplatin-resistant ESCC cells, indicating that targeting MCU may overcome cisplatin resistance. The expression levels of cyclinD1 and Ki-67 represent the changes in the G1 and G2 phases, which are closely related to the malignancy of the tumor and the treatment and prognosis of the patients (30). In the present study, an ESCC xenograft tumor mouse model and a cisplatin-resistant ESCC xenograft tumor mouse model were constructed. Tumor growth was significantly enhanced by cisplatin resistance. Targeting MCU substantially reduced ESCC and cisplatin-resistant ESCC tumor growth. As reflected by the expression of tumor proliferation markers (CyclinD1 and Ki-67), tumor proliferative capacities were markedly increased in cisplatin-resistant ESCC tumors, and this was reversed by MCU inhibition.

Mitochondrial Ca^{2+} homeostasis is pivotal in the regulation of aerobic metabolism and cell survival and plays an important role in the prevention and treatment of cancer metastasis. When the MCU regulates mitochondrial calcium ions, MICU1 and MICU2 can be used as the 'switch' of calcium ions entering mitochondria mediated by MCU. MCU forms a complex structure with MICU1 and MICU2 to regulate the intake of mitochondrial calcium ions, affect the MMP, and participate in the metastasis of cancer cells (31-33). However, the best-known mechanism for cancer metastasis is EMT. In this study, the effect of MCU overexpression or knockout on the expression of EMT-related markers (Vimentin and β-catenin) was assessed. MCU could reverse the occurrence of EMT and reduce the expression of related markers, indicating the role of MCU in the process of cancer metastasis. As previously mentioned, MCU may affect the expression of PD-L1 through MICU1 and MICU2 as well as regulating MMP, highlighting novel possibilities for clinical combination therapy.

Monoclonal antibodies targeting PD-1/PD-L1 have exhibited durable therapeutic responses among patients with ESCC (34). Nevertheless, only a few patients may achieve clinical benefits (35). Previously, neoadjuvant chemotherapy was shown to increase PD-L1 expression in ESCC (36). Cisplatin enhances the antitumor immunity of PD-1/PD-L1 inhibitors in ESCC but upregulates PD-L1 expression in cancer cells (37). Here, the results showed that PD-L1 expression was significantly upregulated in cisplatin-resistant ESCC xenograft tumors compared to ESCC xenograft tumors, indicating that PD-L1 was associated with cisplatin resistance. A recent study found that PD-L1 could enhance cisplatin resistance in gastric cancer (38). MCU knockdown substantially reduced PD-L1 expression in ESCC and cisplatin-resistant ESCC xenograft tumors. The above findings indicated that the interaction between MCU and PD-L1 may promote cisplatin resistance in ESCC. It was hypothesized that MCU may affect the expression of PD-L1 by regulating MICU1, MICU2, and the MMP.

The EMT process may induce cisplatin resistance by transforming relatively motionless epithelial cells into mobile mesenchymal cells and altering cell-cell adhesion and the cellular extracellular matrix, thereby promoting the migration of cancer cells (39,40). The EMT process is reversible and may be modulated through various molecular signals (41). Here, vimentin and β-catenin expression was significantly increased and E-cadherin was markedly decreased in cisplatin-resistant ESCC xenograft tumors, indicating the activation of the EMT process during cisplatin resistance. However, MCU knockdown distinctly impaired the EMT process in cisplatin-resistant ESCC xenograft tumors. This indicated that targeting MCU could mitigate cisplatin resistance in ESCC by suppressing the EMT process.

Angiogenesis during carcinogenesis supplies oxygen and nutrients to proliferative tumor cells, which serves as a therapeutic target against ESCC (42). Silencing oncogenes involved in angiogenesis is required for the treatment of ESCC (43). The results of the present study demonstrated that CD34-labeled

angiogenesis was markedly enhanced in cisplatin-resistant ESCC xenograft tumors and that targeting MCU substantially reduced angiogenesis in ESCC and cisplatin-resistant ESCC xenograft tumors. The results also showed the morphological alterations of microvessels in cisplatin-resistant ESCC and the therapeutic effects of MCU inhibition in targeting angiogenesis in ESCC.

The present study reported for the first time the oncogenic role of MCU in ESCC and demonstrated the inhibitory effect of MCU on tumor growth in cisplatin-resistant and non-cisplatin-resistant ESCC, indicating that MCU knockdown may play an anticancer role by reducing the expression of PD-L1 and EMT markers. Thus, targeting MCU may be a promising therapeutic strategy for the treatment of ESCC.

In conclusion, the results of the present study suggested that knockdown of MCU reduced the proliferation, migration, and MMP in ESCC cell lines and cisplatin-resistant ESCC cell lines. Furthermore, targeting MCU suppressed tumor growth and alleviated cisplatin resistance in ESCC xenograft mouse models. Collectively, these results highlighted a pharmacological strategy in targeting MCU that may be utilized for mitigating cisplatin resistance in ESCC.

Acknowledgements

Not applicable.

Funding

This study was supported by funding from the Natural Science Foundation of Ningxia (grant no. 2021AAC03343), Ningxia Hui Autonomous Region Key Research and Development Plan Project Specification (grant nos. 2020BEG03001 and 2018BEG02007), and the Science Foundation of Inner Mongolia Autonomous Region (grant no. 2020MS08179).

Availability of data and materials

The datasets used and/or analyzed during the present study are available from the corresponding author on reasonable request.

Authors' contributions

YM, XW, FZ, and SY conceived the study, and wrote, revised and edited the manuscript. YL analyzed the data, and wrote, revised, and edited the manuscript. YH and HY performed the experiments and analyzed the data. XM performed the experiments and drafted the manuscript. HL performed the experiments and data analysis. RH and WL performed the experiments and revised the manuscript for intellectual content. XZ performed the experiments and drafted the manuscript. XZ and BCC analyzed the data and revised the manuscript. YM and XW confirm the authenticity of all the raw data. All authors read and approved the final version of the manuscript.

Ethics approval and consent to participate

The protocols used in the present study strictly adhered to the Guidelines for the Care and Use of Laboratory Animals and was approved by the Ethics Committee of Ningxia Medical University (approval no. 2020880).

Patient consent for publication

Not applicable.

Competing interests

The authors declare that they have no competing interests.

References

1. Arnold M, Ferlay J, van Berge Henegouwen MI and Soerjomataram I: Global burden of oesophageal and gastric cancer by histology and subsite in 2018. Gut 69: 1564-1571, 2020.
2. GBD 2017 Oesophageal Cancer Collaborators: The global, regional, and national burden of oesophageal cancer and its attributable risk factors in 195 countries and territories, 1990-2017: A systematic analysis for the global burden of disease study 2017. Lancet Gastroenterol Hepatol 5: 582-597, 2020.
3. van Laarhoven HW: Is chemotherapy for advanced or metastatic oesophageal squamous cell carcinoma no longer needed? Lancet Oncol 21: 743-745, 2020.
4. Hu Y, Xie C, Yang H, Ho JWK, Wen J, Han L, Lam KO, Wong IYH, Law SYK, Chiu KWH, *et al*: Computed tomography-based deep-learning prediction of neoadjuvant chemoradiotherapy treatment response in esophageal squamous cell carcinoma. Radiother Oncol 154: 6-13, 2021.
5. Leng XF, Daiko H, Han YT and Mao YS: Optimal preoperative neoadjuvant therapy for resectable locally advanced esophageal squamous cell carcinoma. Ann N Y Acad Sci 1482: 213-224, 2020.
6. Hsu PK, Yeh YC, Chien LI, Huang CS and Hsu HS: Clinicopathological significance of pathologic complete lymph node regression after neoadjuvant chemoradiotherapy in esophageal squamous cell carcinoma. Ann Surg Oncol 28: 2048-2058, 2021.
7. Chen S, Yang M, Wang C, Ouyang Y, Chen X, Bai J, Hu Y, Song M, Zhang S and Zhang Q: Forkhead box D1 promotes EMT and chemoresistance by upregulating lncRNA CYTOR in oral squamous cell carcinoma. Cancer Lett 503: 43-53, 2021.
8. Chang WM, Chang YC, Yang YC, Lin SK, Chang PM and Hsiao M: AKR1C1 controls cisplatin-resistance in head and neck squamous cell carcinoma through cross-talk with the STAT1/3 signaling pathway. J Exp Clin Cancer Res 38: 245, 2019.
9. Oshimori N, Oristian D and Fuchs E: TGF-β promotes heterogeneity and drug resistance in squamous cell carcinoma. Cell 160: 963-976, 2015.
10. Mohapatra P, Shriwas O, Mohanty S, Ghosh A, Smita S, Kaushik SR, Arya R, Rath R, Das Majumdar SK, Muduly DK, *et al*: CMTM6 drives cisplatin resistance by regulating Wnt signaling through the ENO-1/AKT/GSK3β axis. JCI Insight 6: e143643, 2021.
11. Liu Z, Gu S, Lu T, Wu K, Li L, Dong C and Zhou Y: IFI6 depletion inhibits esophageal squamous cell carcinoma progression through reactive oxygen species accumulation via mitochondrial dysfunction and endoplasmic reticulum stress. J Exp Clin Cancer Res 39: 144, 2020.
12. Xu Y, Wang C, Su J, Xie Q, Ma L, Zeng L, Yu Y, Liu S, Li S, Li Z and Sun L: Tolerance to endoplasmic reticulum stress mediates cisplatin resistance in human ovarian cancer cells by maintaining endoplasmic reticulum and mitochondrial homeostasis. Oncol Rep 34: 3051-3060, 2015.
13. Ren T, Zhang H, Wang J, Zhu J, Jin M, Wu Y, Guo X, Ji L, Huang Q, Zhang H, *et al*: MCU-dependent mitochondrial Ca^{2+} inhibits NAD^{+}/SIRT3/SOD2 pathway to promote ROS production and metastasis of HCC cells. Oncogene 36: 5897-5909, 2017.
14. Cui C, Yang J, Fu L, Wang M and Wang X: Progress in understanding mitochondrial calcium uniporter complex-mediated calcium signalling: A potential target for cancer treatment. Br J Pharmacol 176: 1190-1205, 2019.
15. Vultur A, Gibhardt CS, Stanisz H and Bogeski I: The role of the mitochondrial calcium uniporter (MCU) complex in cancer. Pflugers Arch 470: 1149-1163, 2018.

16. Liu Y, Jin M, Wang Y, Zhu J, Tan R, Zhao J, Ji X, Jin C, Jia Y, Ren T and Xing J: MCU-induced mitochondrial calcium uptake promotes mitochondrial biogenesis and colorectal cancer growth. Signal Transduct Target Ther 5: 59, 2020.
17. Tosatto A, Sommaggio R, Kummerow C, Bentham RB, Blacker TS, Berecz T, Duchen MR, Rosato A, Bogeski I, Szabadkai G, *et al*: The mitochondrial calcium uniporter regulates breast cancer progression via HIF-1α. EMBO Mol Med 8: 569-585, 2016.
18. Stoica SI, Onose G, Pitica IM, Neagu AI, Ion G, Matei L, Dragu LD, Radu LE, Chivu-Economescu M, Necula LG, *et al*: Molecular aspects of hypoxic stress effects in Chronic ethanol exposure of neuronal cells. Curr Issues Mol Biol 45: 1655-1680, 2023.
19. Xue W, Shen Z, Li L, Zheng Y, Yan D, Kan Q and Zhao J: Long non-coding RNAs MACC1-AS1 and FOXD2-AS1 mediate NSD2-induced cisplatin resistance in esophageal squamous cell carcinoma. Mol Ther Nucleic Acids 23: 592-602, 2020.
20. Cui W, Fang T, Duan Z, Xiang D, Wang Y, Zhang M, Zhai F, Cui X and Yang L: Dihydroartemisinin sensitizes esophageal squamous cell carcinoma to cisplatin by inhibiting sonic hedgehog signaling. Front Cell Dev Biol 8: 596788, 2020.
21. Wang J, Ji H, Zhu Q, Yu X, Du J and Jiang Z: Co-inhibition of BMI1 and Mel18 enhances chemosensitivity of esophageal squamous cell carcinoma *in vitro* and *in vivo*. Oncol Lett 17: 5012-5022, 2019.
22. Barra GB, Santa Rita TH, Almeida ALSC, Jácomo RH and Nery LFA: Serum has higher proportion of Janus kinase 2 V617F mutation compared to paired EDTA-whole blood sample: A model for somatic mutation quantification using qPCR and the 2 method. Diagnostics (Basel) 10: 153, 2020.
23. Sugimura K, Yamasaki M, Yasuda T, Yano M, Hirao M, Fujitani K, Kimura Y, Miyata H, Motoori M, Takeno A, *et al*: Long-term results of a randomized controlled trial comparing neoadjuvant Adriamycin, cisplatin, and 5-fluorouracil vs docetaxel, cisplatin, and 5-fluorouracil followed by surgery for esophageal cancer (OGSG1003). Ann Gastroenterol Surg 5: 75-82, 2020.
24. Liu H, Zhang J, Luo X, Zeng M, Xu L, Zhang Q, Liu H, Guo J and Xu L: Overexpression of the long noncoding RNA FOXD2-AS1 promotes cisplatin resistance in esophageal squamous cell carcinoma through the miR-195/Akt/mTOR axis. Oncol Res 28: 65-73, 2020.
25. Suo D, Wang L, Zeng T, Zhang H, Li L, Liu J, Yun J, Guan XY and Li Y: NRIP3 upregulation confers resistance to chemoradiotherapy in ESCC via RTF2 removal by accelerating ubiquitination and degradation of RTF2. Oncogenesis 9: 75, 2020.
26. Zhou T, Fu H, Dong B, Dai L, Yang Y, Yan W and Shen L: HOXB7 mediates cisplatin resistance in esophageal squamous cell carcinoma through involvement of DNA damage repair. Thorac Cancer 11: 3071-3085, 2020.
27. Ben-David U, Siranosian B, Ha G, Tang H, Oren Y, Hinohara K, Strathdee CA, Dempster J, Lyons NJ, Burns R, *et al*: Genetic and transcriptional evolution alters cancer cell line drug response. Nature 560: 325-330, 2018.
28. PCAWG Transcriptome Core Group; Calabrese C, Davidson NR, Demircioğlu D, Fonseca NA, He Y, Kahles A, Lehmann KV, Liu F, Shiraishi Y *et al*: Genomic basis for RNA alterations in cancer. Nature 578: 129-136, 2020.
29. Wang X, Song X, Cheng G, Zhang J, Dong L, Bai J, Luo D, Xiong Y, Li S, Liu F, *et al*: The regulatory mechanism and biological significance of mitochondrial calcium uniporter in the migration, invasion, angiogenesis and growth of gastric cancer. Onco Targets Ther 13: 11781-11794, 2020.
30. Xu P, Zhang X, Ni W, Fan H, Xu J, Chen Y, Zhu J, Gu X, Yang L, Ni R, *et al*: Upregulated HOXC8 expression is associated with poor prognosis and oxaliplatin resistance in hepatocellular carcinoma. Dig Dis Sci 60: 3351-3363, 2015.
31. Kamer KJ, Jiang W, Kaushik VK, Mootha VK and Grabarek Z: Crystal structure of MICU2 and comparison with MICU1 reveal insights into the uniporter gating mechanism. Proc Natl Acad Sci USA 116: 3546-3555, 2019.
32. Patron M, Checchetto V, Raffaello A, Teardo E, Vecellio Reane D, Mantoan M, Granatiero V, Szabò I, De Stefani D and Rizzuto R: MICU1 and MICU2 finely tune the mitochondrial Ca2+ uniporter by exerting opposite effects on MCU activity. Mol Cell 53: 726-737, 2014.
33. Wang C, Jacewicz A, Delgado BD, Baradaran R and Long SB: Structures reveal gatekeeping of the mitochondrial Ca^{2+} uniporter by MICU1-MICU2. Elife 9: e59991, 2020.
34. Lee J, Kim B, Jung HA, La Choi Y and Sun JM: Nivolumab for esophageal squamous cell carcinoma and the predictive role of PD-L1 or CD8 expression in its therapeutic effect. Cancer Immunol Immunother 70: 1203-1211, 2021.
35. McBride S, Sherman E, Tsai CJ, Baxi S, Aghalar J, Eng J, Zhi WI, McFarland D, Michel LS, Young R, *et al*: Randomized phase II trial of nivolumab with stereotactic body radiotherapy versus nivolumab alone in metastatic head and neck squamous cell carcinoma. J Clin Oncol 39: 30-37, 2021.
36. Fukuoka E, Yamashita K, Tanaka T, Sawada R, Sugita Y, Arimoto A, Fujita M, Takiguchi G, Matsuda T, Oshikiri T, *et al*: Neoadjuvant chemotherapy increases PD-L1 expression and $CD8^+$ tumor-infiltrating lymphocytes in esophageal squamous cell carcinoma. Anticancer Res 39: 4539-4548, 2019.
37. Tran L, Allen CT, Xiao R, Moore E, Davis R, Park SJ, Spielbauer K, Van Waes C and Schmitt NC: Cisplatin alters antitumor immunity and synergizes with PD-1/PD-L1 inhibition in head and neck squamous cell carcinoma. Cancer Immunol Res 5: 1141-1151, 2017.
38. Wu L, Cai S, Deng Y, Zhang Z, Zhou X, Su Y and Xu D: PD-1/PD-L1 enhanced cisplatin resistance in gastric cancer through PI3K/AKT mediated P-gp expression. Int Immunopharmacol 94: 107443, 2021.
39. Zhu X, Chen L, Liu L and Niu X: EMT-mediated acquired EGFR-TKI resistance in NSCLC: Mechanisms and strategies. Front Oncol 9: 1044, 2019.
40. Ashrafizadeh M, Zarrabi A, Hushmandi K, Kalantari M, Mohammadinejad R, Javaheri T and Sethi G: Association of the epithelial-mesenchymal transition (EMT) with cisplatin resistance. Int J Mol Sci 21: 4002, 2020.
41. Shen M, Xu Z, Xu W, Jiang K, Zhang F, Ding Q, Xu Z and Chen Y: Inhibition of ATM reverses EMT and decreases metastatic potential of cisplatin-resistant lung cancer cells through JAK/STAT3/PD-L1 pathway. J Exp Clin Cancer Res 38: 149, 2019.
42. Chen Y, Wang D, Peng H, Chen X, Han X, Yu J, Wang W, Liang L, Liu Z, Zheng Y, *et al*: Epigenetically upregulated oncoprotein PLCE1 drives esophageal carcinoma angiogenesis and proliferation via activating the PI-PLCε-NF-κB signaling pathway and VEGF-C/Bcl-2 expression. Mol Cancer 18: 1, 2019.
43. Mao Y, Wang Y, Dong L, Zhang Y, Zhang Y, Wang C, Zhang Q, Yang S, Cao L, Zhang X, *et al*: Hypoxic exosomes facilitate angiogenesis and metastasis in esophageal squamous cell carcinoma through altering the phenotype and transcriptome of endothelial cells. J Exp Clin Cancer Res 38: 389, 2019.